

On the intermittency of hot plasma loops in the solar corona

PHILIP G. JUDGE¹ AND N. PAUL M. KUIN²

¹ *Visitor, Astronomical Institute of the University of Bern, Sidlerstrasse 5, 3012 Bern, and
High Altitude Observatory, National Center for Atmospheric Research, Boulder CO 80307-3000, USA*

² *Mullard Space Science Laboratory, University College London, Holmbury St. Mary, Dorking RH5 6NT, UK*

(Dated: Accepted . Received ; in original form)

ABSTRACT

A recent analysis has suggested that the heating of plasma loops in the solar corona depends not just on the Poynting flux but also on processes yet to be identified. This discovery reflects and refines earlier questions such as, why and how are entire hydromagnetic structures only intermittently loaded with bright coronal plasma (Litwin & Rosner 1993)? The present work scrutinizes more chromospheric and coronal data, with the aim of finding reproducible observational constraints on coronal heating mechanisms. Six independent scans of chromospheric active region magnetic fields are investigated and correlated to overlying hot plasma loops. For the first time, the footpoints of over 30 bright plasma loops are thus related to scalar proxies for the Poynting fluxes measured from the upper chromosphere. Although imperfect, the proxies all indicate a general lack of correlation between footpoint Poynting flux and loop brightness. Our findings consolidate the claim that unobserved physical processes are at work which govern the heating of long-lived coronal loops.

Keywords: Solar corona

1. INTRODUCTION

Sometimes in a mature research field, there is a need to step back and re-assess some fundamental facts. The present paper aims to establish a clearer observational picture of the physical connection between the magnetic field near the coronal base, particularly the Poynting flux, and bright coronal plasma. For decades correlations have been found between photospheric magnetic fluxes and X-ray brightness of the corona (examples include Krieger et al. 1971; Poletto et al. 1975; Golub et al. 1980; Schrijver & Harvey 1989; Schrijver & Zwaan 2000; Pevtsov et al. 2003; Barczynski et al. 2018; Toriumi & Airapetian 2022). It has long been established that the solar X-ray corona above active regions consists of multiple loop-like structures, heated somehow through the magnetic fields confining them (e.g. van Speybroeck et al. 1970; Rosner et al. 1978). These are now believed to consist of “tubes” of hot plasma, with amorphous cross sections, aligned within magnetic flux surfaces and extending upwards from strongly magnetized regions in the lower atmosphere (Malanushenko et al. 2022). The

simple fact that we clearly see such structures begs the question of what organizes the plasma into loops on observable scales (Rosner 1990; Litwin & Rosner 1993. The latter we refer to as “LW93”). Why are certain tubes, parts of large hydromagnetic structures, so full of hot plasma and others not?

This problem presents potential challenges for typical thermal models which, for a given upward flux of electromagnetic energy dissipated in the corona, produce unique and deterministic equilibria (see the intriguing history of 1D and 0D modeling in articles by Kuin & Martens 1982; McClymont & Craig 1985a,b; Craig & Schulkes 1985; van den Oord & Barstow 1988; Craig 1990; Martens 2010; Cargill et al. 2012a). Under the current picture of coronal heating, dissipative structures exist only on small scales below ~ 200 km, perhaps approaching kinetic scales of tens of meters (Judge & Ionson 2024). Some have proposed, based in part on this picture, that unresolved threads or ribbons of plasma within loops dominate the emission from within each loop (Aschwanden et al. 2000; Patsourakos & Klimchuk 2005; Klimchuk 2006; Aschwanden et al. 2007; Klimchuk et al. 2008; López Fuentes & Klimchuk 2022). But then one faces the question of why the heated plasma

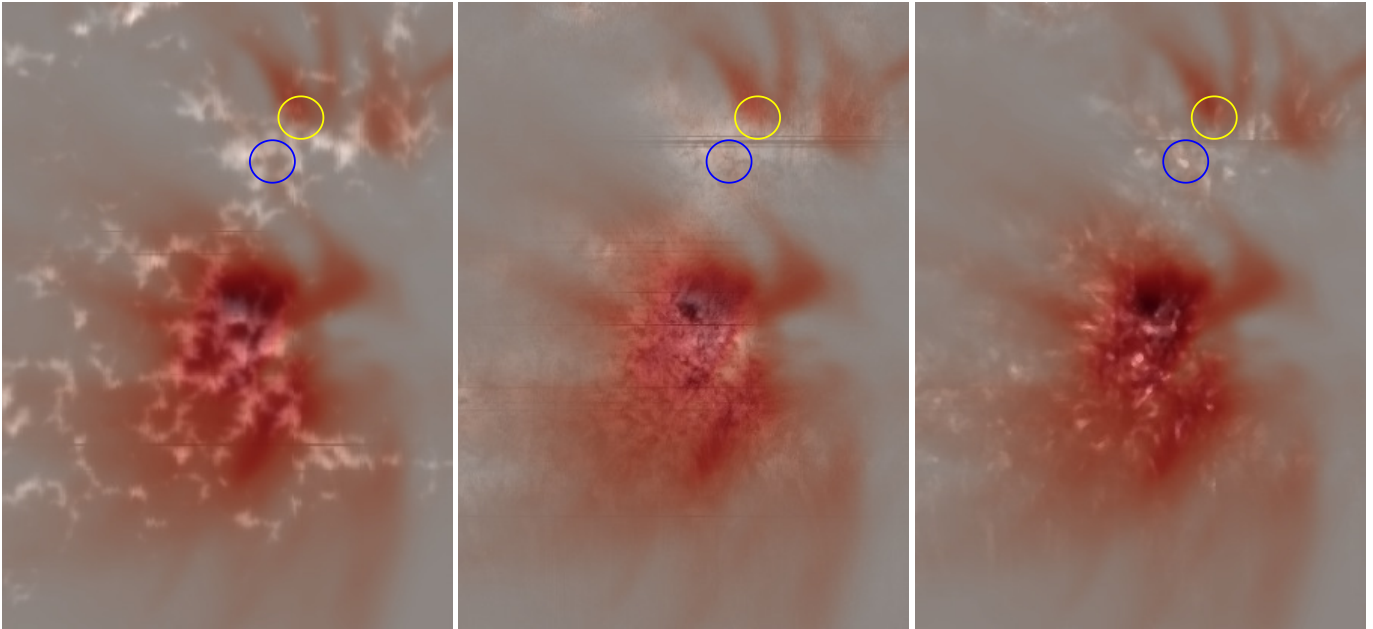


Figure 1. Line of sight photospheric magnetic fields (left column), chromospheric magnetic fields (middle), and scalar proxy (expression 7) of Poynting flux (right) are rendered in grayscale for data from the GRIS instrument at the GREGOR telescope, on 28 September 2020 (see J24b for details). The region is centered near $X = -13$, $Y = 325$ in heliographic coordinates. The photospheric line of Si I $\lambda 1082.5$ nm, and chromospheric blended lines of He I at 1083.0 nm were used to derive the quantities shown. Superposed in red are negative images of the footpoints of coronal loops as seen in the AIA 17.1 nm channel, which have very similar morphology to other AIA channels (J24b). The field of view is $40''.5 \times 60''.5$, set by the area scanned by the GRIS slit. The yellow circled region is the footpoint of a hot plasma loop base, the otherwise similar underlying region, circled in blue, is not.

simultaneously exists both on fine scales, yet is also organized on the larger observable scales, which currently exceed ~ 200 km at EUV wavelengths (Rachmeler et al. 2022). Is the upward Poynting flux organized on such scales? Recent findings of Judge et al. (2024a), henceforth “J24a”, based upon data of one active region, suggest not. Instead these authors speculated that the corona itself might regulate its own rate of heating, an idea with origins in some theoretical work (Uzdensky 2007; Einaudi et al. 2021).

J24a analyzed chromospheric magnetic fields using the ViSP instrument (de Wijn et al. 2022) to measure states of polarization of the 854.2 nm line of Ca II at the Daniel K. Inouye Solar Telescope (“DKIST”, Rimmele et al. 2020). These data were compared with space-based measurements of overlying coronal plasmas. Quantities related to the upward Poynting flux at the base of coronal plasma loops were found to be essentially uncorrelated with the brightness of footpoints of heated plasmas observed with the EUV channels of the AIA instrument (Lemen et al. 2012) on SDO (Pesnell et al. 2012). Such a result, if confirmed, would represent a new fundamental fact with which to test coronal heating mechanisms.

The main purpose of the present paper is to find further observational evidence for or against this result.

Our approach is to use chromospheric measurements of magnetic and thermodynamic structure to estimate crudely the likely variation of Poynting flux across the surface immediately beneath the coronal loops. Measurements of chromospheric magnetic fields well above the $\beta = 1$ surface avoids some of the difficulties associated with measurements of photospheric magnetic fields, but at the expense of sacrificing any information on magnetic field components transverse to the line of sight. In the present paper we study four additional ViSP scans that were not reported in J24a, along with a higher angular resolution scan in the infrared region from the GRIS spectropolarimeter on the GREGOR telescope (Judge et al. 2024b, henceforth “J24b”). Both photospheric and chromospheric lines were observed by these instruments, building maps of surface conditions by scanning perpendicular to the slit. Consequently, velocity measurements, like the Zeeman measurements of chromospheric magnetic fields, are restricted to components along the line-of-sight. Some theoretical ideas are then pitted against these data in section 4.

2. POYNTING VECTORS AND SCALAR PROXIES

2.1. Approximations

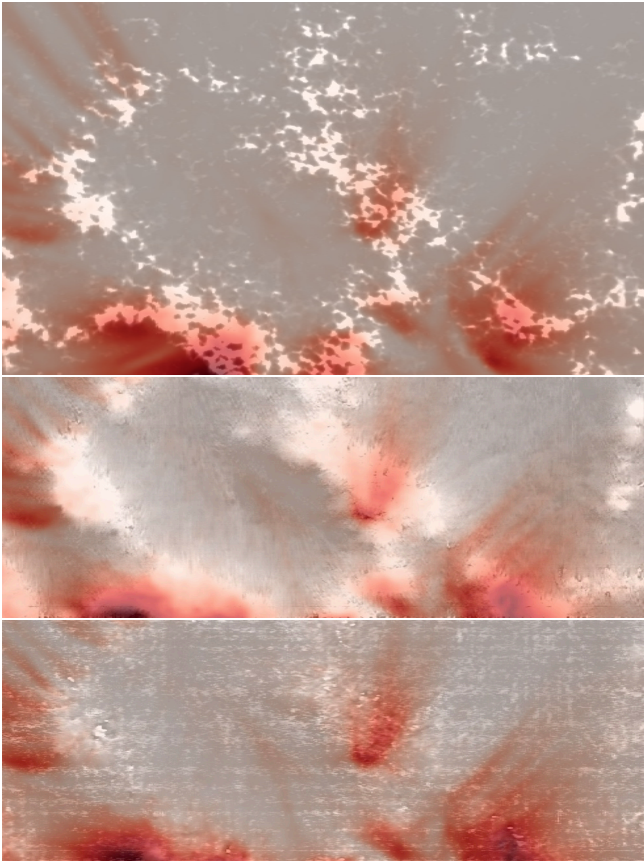


Figure 2. Line of sight photospheric magnetic fields (top row), chromospheric magnetic fields (middle row), and scalar proxy of Poynting flux (bottom row, from expression 7) are rendered in grayscale for DKIST dataset BRWJV+AVORO (J24a), two scans centered at 3-Jun-2022 17:52:23 at $X = -411$, $Y = 377$. The photospheric lines of Fe I near 6302 nm, and chromospheric line of He I at 854.2 nm were used to derive the quantities shown. Superposed in red are negative images of the footpoints of coronal loops as seen in the AIA 17.1 nm channel. Owing to the different magnifications of the two arms of the ViSP spectrograph used, the photospheric field has a field of view of $100'' \times 77''$, the other images $100'' \times 50''$.

In J24a and J24b, scalar “proxies” for Poynting vectors were used as first, crude estimates of the upward-directed Poynting flux emerging from the upper chromosphere into the corona. In ideal MHD, the Poynting vector is

$$\mathbf{S} = -\frac{c}{4\pi}(\mathbf{u} \times \mathbf{B}) \times \mathbf{B}. \quad (1)$$

Projecting the fluid velocity vector \mathbf{u} into components perpendicular and parallel to the magnetic field \mathbf{B} , which has unit vector $\hat{\mathbf{b}}$,

$$\mathbf{u}_{\perp} = (\hat{\mathbf{b}} \times \mathbf{u}) \times \hat{\mathbf{b}}; \quad \mathbf{u}_{\parallel} = \mathbf{u} - \mathbf{u}_{\perp},$$

then (1) is simply

$$\mathbf{S} = \frac{c}{4\pi} B^2 u \hat{\mathbf{u}}_{\perp}. \quad (2)$$

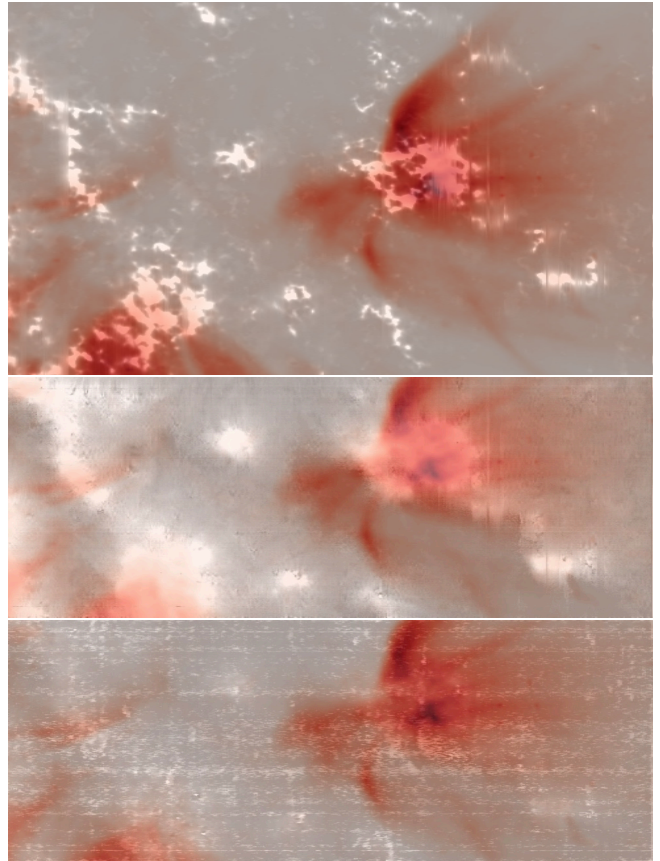


Figure 3. Magnetic and coronal properties are shown as in Figure 2, except for DKIST dataset AODMM+APJND. The mid time of the scan was 2-Jun-2022 20:02:23, it was centered near $X = -495$, $Y = 495$.

Clearly \mathbf{S} is perpendicular to \mathbf{B} , and $S = |\mathbf{S}| \leq \frac{c}{4\pi} B^2 u$.

In comparison, our measurements of Doppler profiles and Zeeman effect yield only scalar quantities

$$u_{\text{LOS}} = \mathbf{u} \cdot \hat{\mathbf{k}}, \quad \text{and} \quad (3)$$

$$B_{\text{LOS}} = \mathbf{B} \cdot \hat{\mathbf{k}}, \quad (4)$$

where unit vector $\hat{\mathbf{k}}$ lies along the line of sight. Therefore, based upon equation (2), in J24a, we compared estimates of $S = |\mathbf{S}|$ with intensities of the coronal emission immediately above, using the crude scaling

$$S \propto B_{\text{LOS}}^2 u_{\text{LOS}}, \quad (5)$$

and a scaling appropriate for Alfvén waves (expression 7 below), with u_{LOS} measured from Doppler widths and shifts of the cores of chromospheric lines. Relation (5) assumes that some unknown but small fraction of the total magnetic energy flux (equation 2) is available for coronal heating. J24a showed that this quantity varied across the solar surface similarly to estimates using the scaling (7) for Alfvén waves. Therefore, only the latter are shown in the present paper.

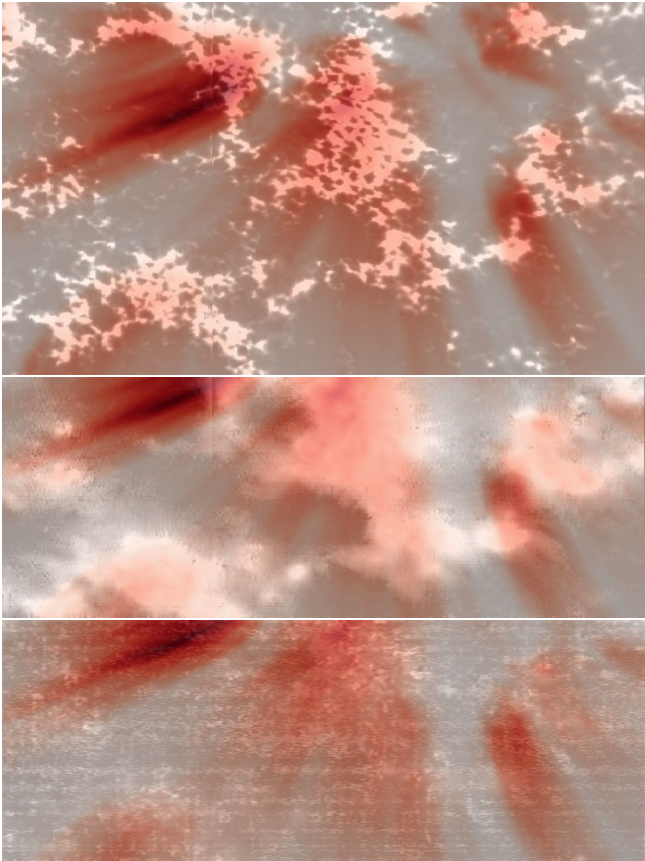


Figure 4. Magnetic and coronal properties are shown as in Figure 2, except for scans AWOWP+AXVLY, with a mid time of 23 June 2023 17:23:21, centered near $X = -416$, $Y = -436$.

2.2. Assumptions and limitations

The magnitude of S depends on geometrical relations between vectors \mathbf{B} and \mathbf{u} , which we cannot measure at present. So we face two choices: first acknowledge that the observational data are inadequate to make further progress, and stop. Second, make explicit assumptions:

1. u_{LOS} contains information on u_{\perp} , and
2. statistical correlations between chromospheric \mathbf{u} and \mathbf{B} are similar in the neighborhood of the footpoints of coronal plasma loops.

The latter is an hypothesis eventually to be tested, prompted by the observed universal presence of non-thermal, unresolved motions in the chromosphere.

Equations (1) and (2) relate only solar properties, where vectors \mathbf{u} and \mathbf{B} are independent. Equations (3) and (4) relate these two vectors to an entirely different vector $\hat{\mathbf{k}}$ defined by the line of sight. For almost all lines of sight, it must be the case that the independent measurements of u_{LOS} and B_{LOS} will always yield information about S , except in three singular cases: (a)

\mathbf{u} is parallel to \mathbf{B} , (b) \mathbf{u} is perpendicular to $\hat{\mathbf{k}}$, and (c) \mathbf{B} is perpendicular to $\hat{\mathbf{k}}$. Cases (b) and (c) are statistically rare, $\hat{\mathbf{k}}$ being entirely unrelated to the solar vectors. Further, local verticals on the Sun are at least 0.33 radians from the observed LOS during all scans presented below (heliographic coordinates are listed in the figure captions). The local magnetic fields are statistically significantly inclined to the LOS, i.e. at least the singular case $\mathbf{B} \cdot \hat{\mathbf{k}} = 0$ is a rare occurrence.

However, for strictly field-aligned flows (case a), our analysis will lead to spurious non-zero estimates of S . Such flows certainly contribute to Doppler signals used below, potentially leading to systematic errors in our analysis. But two arguments suggest that such errors are not overwhelming. First, if our assumption 2. is valid, they will contribute only a statistically constant offset in S across the observed fields of view. Therefore we can partly justify relating overlying coronal emission to systematic changes in S across the field of view. Secondly such macroscopic flows along fibrils are generally significantly less than unresolved motions contributing to widths of chromospheric lines (e.g. Athay 1976).

2.3. Alfvén waves

The remaining significant motions contributing to S are associated with Alfvén and fast modes, recalling that MHD turbulence is the non-linear interaction of Alfvén waves. We estimate the Poynting flux as the product of the wave group speed $c_A \sim B/\sqrt{4\pi\rho}$ with $B \sim B_{\text{LOS}}$ and wave energy densities. The Alfvén waves carry an energy density along the ambient magnetic field \mathbf{B}_0 of

$$\varepsilon = \frac{B_1^2}{4\pi} = \rho u_1^2 \quad (6)$$

where B_1 and u_1 are the amplitudes of magnetic and velocity perturbations perpendicular to \mathbf{B}_0 (Braginskii 1965). Velocity perturbations u_1^2 can be estimated from the non-thermal widths of chromospheric lines, which tend to exceed statistical fluctuations in Doppler shifts of line centroids. We therefore examine the proxy (Jordan et al. 1984, 1987):

$$S \propto \frac{B_{\text{LOS}}}{\sqrt{4\pi\rho}} \rho \xi^2, \quad (7)$$

using non-thermal spectral line widths ξ to estimate u_1 . The densities of the plasma at the formation heights of the Ca II and He I line cores are given in J24a,b. Many observations show that ξ in chromospheric lines statistically increases towards the solar limb (Linsky & Avrett 1970, see their page 180), a behavior compatible with wave motions transverse to statistically radial magnetic fields within coronal loop footpoints.

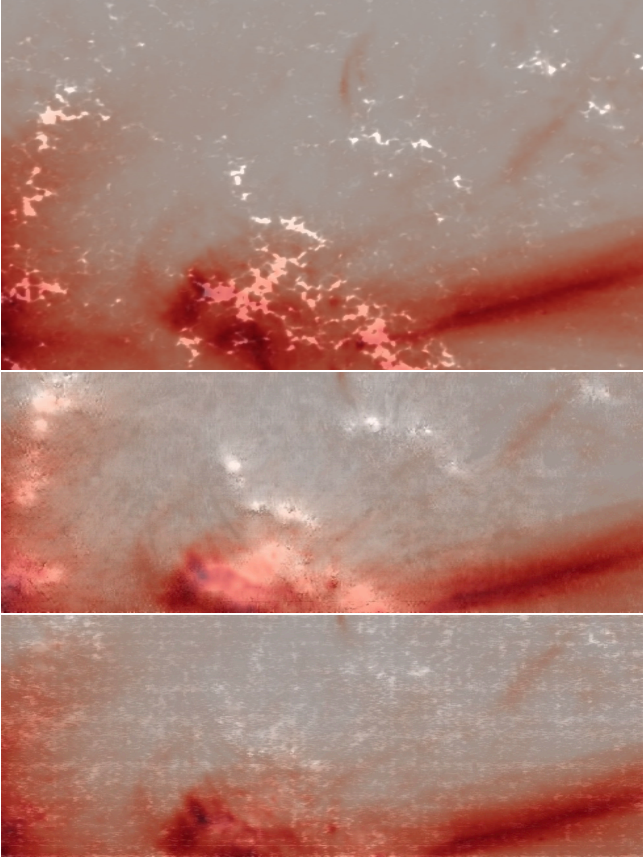


Figure 5. Magnetic and coronal properties are shown as in Figure 2, except for DKIST dataset BPJDD+BQKZZ, obtained at midtime 18:21:07 on Jun 23 2023. $X = -312$, $Y = -377$.

3. RECENT MEASUREMENTS OF CHROMOSPHERIC MAGNETIC FIELDS

We analyze data from two ground-based observatories to complement the analysis of J24a, which was concerned with just one scan of ViSP chromospheric magnetism in relation to data from the HMI (Hoeksema et al. 2018) and AIA instruments on SDO, and the IRIS UV instrument (Lemen et al. 2011). Here we examine chromospheric magnetic fields measured closer still to the base of the corona, by studying the 1083 nm line of He I, and also analyze data from the four other scans in Ca II obtained during the series of observations reported by J24a.

The Ca II line core forms just ~ 2 pressure scale heights beneath the corona (Cauzzi et al. 2008; Leenaarts et al. 2009), 8-9 pressure scale heights above the photosphere. With lower limits to field strengths measured here of ~ 200 G, the plasma $\beta = 1$ surface will be $\lesssim 400$ km, $\lesssim 3$ pressure scale heights, above the photosphere.

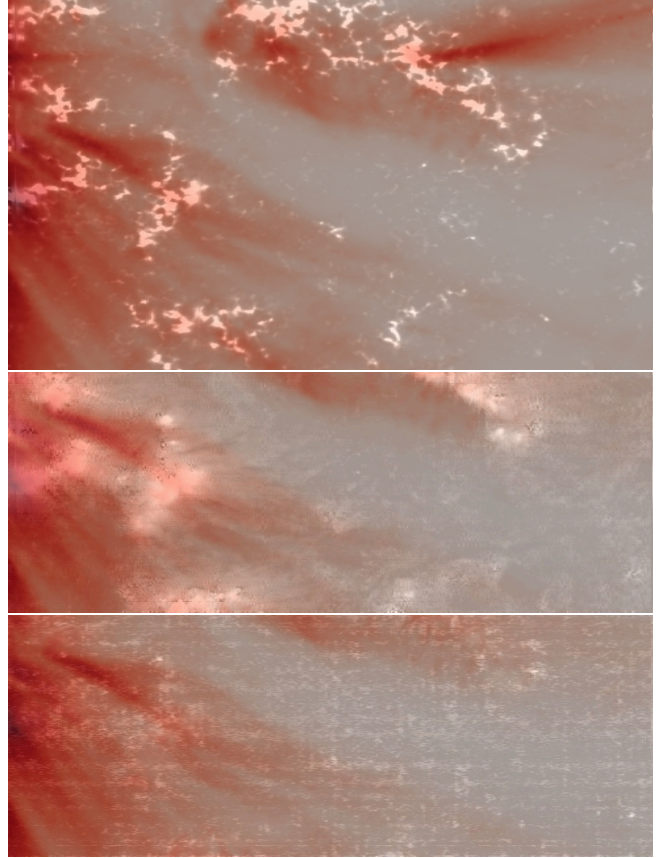


Figure 6. Magnetic and coronal properties are shown as in Figure 2, except for dataset DKIST BNKVM+BODXM, obtained at midtime 18:49:52 on Jun 23 2023, centered at $X = 412$ $Y = 439$.

The lines of the He I 1083 nm multiplet core form in tenuous and dynamic plasma close to the base of the corona, mostly above the stratified chromosphere, where ionizing radiation can excite levels within the triplet system of helium (Leenaarts et al. 2016).

3.1. GRIS data from 28 September 2020

J24b analyzed data from the GRIS instrument (Colados et al. 2012) on the GREGOR telescope (Schmidt et al. 2012; Kleint et al. 2020), but using the lines of Si I 1082.7 and He I 1083 nm from the GREGOR telescope. These infrared data were acquired by Tobias Felipe and Christoph Kuckein on 28 Sep 2020, they are discussed in detail by J24b. Figure 1 shows magnetic fields derived from the GRIS scan in lines of Si I at 1082.7 and He I at 1083.0 nm. The Si I line forms at 200-500 km above the continuum photosphere (Judge et al. 2014). Using the measured non-thermal linewidth ξ in place of u_{LOS} in equation (7), $S \propto \rho \xi^2 c_A$ is shown in the rightmost panel of Fig. 1, and in the lowest rows of all other figures. For reference P24b used $\rho \sim 10^{-13}$ g cm $^{-3}$ as an estimate of the plasma mass density at the formation height of

He I 1083 nm (Avrett et al. 1994). In this and later figures the heliographic solar X and Y coordinates are given. The angle between lines of sight and local vertical on the Sun is 0.33 radians for Figure 1, and up to 0.74 radians for the ViSP scans in later figures. Only *differences* between these estimates across the solar surface can be assumed to be meaningful.

The lowest panel of Figure 1 is morphologically similar to a figure, not shown here, of the other Poynting flux scalar. Both figures demonstrate the fact that *no correlation is found between coronal plasma loop footpoints and underlying chromospheric B_{LOS} magnetic fields and proxies for Poynting flux*. For example, the yellow circle identifies a loop footpoint, the blue circle a region of stronger magnetic field and Poynting flux with no associated loop footpoint. These are just two of many examples.

This lack of correlation does not depend on projection effects or the small uncertainties ($\sim \pm 2''$, J24b) in co-alignment. The GRIS data are for an active region which is inclined at ≈ 0.33 radians to the LOS. The difference in formation height between 1800 km near where the Ca II and He I line cores are formed, and the onset of 17.1 nm mission is ≈ 1 Mm in conductively coupled models (e.g. Hansteen 1993). Therefore a vertical plasma loop would appear displaced by $\pm \sim 0.7$ Mm ($< 1''$) from the chromosphere along the (unknown) tube’s field lines. This offset is smaller than the estimated co-alignment accuracy. However, photospheric images would be displaced in projection by ~ 2.5 Mm.

3.2. DKIST data from 02-03 June 2022

J24a focused on just one scan with the ViSP instrument obtained on 3 June 2022. Data of the 630 nm Fe I line pair and the 854.2 nm chromospheric line of Ca II were used to extract properties of the plasma and magnetic field. Four similar ViSP scans were made between June 2 2022 20:02 and June 3 18:50 UT (see Table 1 of J24a). All data were analyzed with co-aligned supporting data from instruments on the SDO spacecraft. In Figures 3 - 6, data from the remaining four scans are shown in a similar manner to Figure 2. Measured LOS chromospheric magnetic flux densities over the photospheric flux concentrations are typically 250 Mx cm^{-2} (J24a, J24b). Clearly the behavior found by J24a is *typical of all these cases*, uncovered through measurements of lines of Fe I at 630 nm and Ca II at 854 nm, formed at roughly 250 and 1500 km above the continuum photosphere respectively (Grec et al. 2010; Cauzzi et al. 2008).

4. DISCUSSION

Six separate scans show that coronal plasma loop footpoints connect to a small area of broader chromospheric

magnetic fluxes beneath. All scans contain 5-6 plasma loop footpoints. Of these ≈ 30 footpoints, the probability that we missed strong correlations of loops with enhanced Poynting fluxes all at the “other” (unobserved) footpoint is negligible ($\sim 0.5^{30}$). The footpoints do tend to lie close to the edges of patches of chromospheric magnetic fields. The same is not true for the plasmas emitting transition region radiation (J24a documented this observation, which included transition region data from IRIS as well as SDO in section 3.3 and their Appendix). These statistically robust results present new and essential observational information concerning conditions at the footpoints of typical active region coronal loops.

While secular motions u_{\perp} driving magnetic fields send energy into the corona (e.g. Parker 1988), higher frequency contributions to S can be reduced. In a homogeneous 1D model, $\gtrsim 50\%$ of the wave power can be reflected analogously to an open boundary on an oscillating string, because of the steep density gradient at the 1D transition region (Wentzel 1978). But less coherent waves in an inhomogeneous medium can intermingle, become non-linear, leading to a richer variety of phenomena (Wentzel 1978, a modern perspective is summarized by Cranmer & Molnar 2023). In this paper we have assumed that statistically, a constant fraction of any Alfvén wave energy emerges through the transition region, no matter how complex the dynamics. This assumption is questionable. But we note that the structure of transition region plasma remains poorly understood (see J24a,b, also Judge & Ionson 2024), and that the overlying corona and transition region are *products* of the unknown energy transport emerging from the chromosphere. Thus their structure may well differ from a prescribed solution to a steady, 1D energy equation, previously used to analyze reflection coefficients.

4.1. The new observations in context

In spite of trade-offs noted above, the direct physical connection of the chromosphere to the corona is but one reason that chromospheric data are superior to photospheric measurements, for connecting lower to upper atmospheric structures. Another is that *observations are superior to magnetic field extrapolations*, particularly given that between photosphere and chromosphere lies the awkward transition from fluid- to magnetic- dominated stresses near the $\beta = 1$ surface.

All six scans of chromospheric magnetic fields support one elementary fact: *something missing from current observational capabilities must be an important ingredient in the way the corona is heated*. Only a small fraction of the area covered by $|B| \gtrsim 200 \text{ Mx cm}^{-2}$ unipolar chromospheric fields correspond to coronal loop footpoints.

LW93 recognized this problem during an era when only photospheric magnetic fields were routinely measured, at significantly lower angular resolutions:

“Why are coronal loops “rare”, in the sense that only a small subset of coronal magnetic field lines become loaded with hot plasma?...The relative rarity of coronal loops implies that, whatever the heating mechanism, it must have a relatively high threshold so that conditions for its onset are satisfied only in a small fraction of the available coronal volume.”

The existence of a high threshold for the “turn-on” of coronal heating appears at odds with much work on the thermal physics of coronal loops cited earlier. Field-aligned, one dimensional hydrodynamic calculations driven by various kinds of ad-hoc heating parameters, and subject to different formulations for radiation losses, tend to exhibit simple evolution towards unique equilibrium states. Only under special prescribed conditions, namely enhanced heating rates close to footpoints, can exhibit limit-cycle behavior (e.g. Müller et al. 2003b; Martens 2010) as first found in fieldline-integrated thermodynamic calculations of Kuin & Martens (1982). One might also postulate that time-dependent driving of the loop system naturally leads to diverse observed loop properties (e.g. Hansteen 1993). It remains to be seen if, statistically, the observed independence of footpoint brightness from estimates of Poynting flux is consistent with this kind of interpretation.

The present analysis should be understood in terms of the response of the solar upper atmosphere to forcing from a convectively-dominated atmosphere below. In this sense it differs from analyses of data associated with “plumes” or loops originating in the umbrae of sunspots (Foukal 1975, 1976; Chitta et al. 2016), for which convection is suppressed. Our analysis is therefore more applicable to the more general heating problem than special cases for sunspot umbrae (e.g. Foukal 1975), which Ionson (1978) modeled in terms of the resonant absorption picture, which continues to be studied via numerical experimentation (e.g. Beliën et al. 1999; Howson et al. 2020).

4.2. *Locally multipolar fields, reconnection and plasma heating*

The tendency for loop footpoints to appear towards the edges of chromospheric network naturally suggests that reconnection with minority polarity internetwork fields might supply energy for the heating of these loops (Title & Schrijver 1998; Priest et al. 2002; Wang 2016;

Chitta et al. 2017, 2023). Curiously, several inferences from the observations of the chromosphere under the loop footpoints suggest otherwise. In the Appendix we argue that magnetic fields under the observed plasma loops must be unipolar, supporting only small-angle discontinuous fields, in order to satisfy observational data along with force balance.

The plasma β is $\lesssim 0.002$ in the topmost scale height of the chromosphere, using $B_0 \gtrsim 250\text{G}$ from our line-of-sight measurements and a plasma pressure of 4 dyne cm^{-2} from model F of Vernazza et al. (1981). Consequently the intrinsic magnetic field strength B_0 must be nearly constant there, in order to maintain horizontal pressure balance. Along with the relatively uniform measurements of B_{LOS} , this condition leads to a contradiction, denying a role for such reconnection at the foot of the plasma loops.

4.3. *One Poynting flux, two outcomes?*

The two proxies used both by J24a and J24b for the scalar amplitude of the Poynting flux S are far from satisfactory. Not even the sign of the vertical flux can be inferred. The chromospheric network characterized by $B_{\text{LOS}} \gtrsim 200\text{ Mx cm}^{-2}$ occupies several thousand pixels in each scan. Therefore local averages can be used to compare relative sizes of the proxies between regions near plasma loop footpoints and other regions. It is only in this sense that we might claim that S does not change much across the bright network boundaries. If we accept this rationale, then all of the figures show that something not encoded in the data presented has primary control of the overlying corona (J24a), of overlying loops would have emerged. For otherwise some relation between S and the brightness overlying loops would have emerged. Theoretically, the question of what might be responsible for the behavior has followed two trains of thought, discussed next: First, both static and hydro-dynamic thermal models with parameterized heating rates have been studied for the presence of multiple long-lived solutions. Second, instabilities of dissipative structures, be they of MHD or electrostatic origin (LW93), have been studied.

4.3.1. *Thermal models*

Can purely thermal models lead to different long-lived states of coronal loops for the same dissipated Poynting flux? By “thermal” we refer to single fluid, field-aligned hydrodynamics energy transport along a one dimensional representation of a plasma loop (Boris & Mariska 1982; Mariska et al. 1982; Hansteen 1993; Bradshaw & Mason 2003; Bradshaw & Cargill 2013). On surveying the literature, the consensus seems to be “no”, except under certain special conditions (Müller et al. 2003a;

Martens 2010). “Zero-dimensional” studies in which the energy equation is integrated analytically along the loop have also been useful, revealing two kinds of long-lived structures, although not without some initial confusion (Kuin & Martens 1982; Craig & Schulkes 1985). More recent formulations have resolved the differences in favor of evolution towards single equilibria (van den Oord & Barstow 1988; Klimchuk et al. 2008; Cargill et al. 2012b,a). Following Rosner et al. (1978) most such calculations adopt parameterized forms of volumetric heating functions, typically

$$\dot{E} \sim T^a n^b f(s) \quad (8)$$

where T and n are plasma temperature and density, respectively, and s distance along the loop. With “reasonable” values of $|a|$ and $|b|$ less than, say, 2-3, the solutions are unique for given rates of heating \dot{E} . One stabilizing process is a strong exchange of mass and energy between the stratified chromosphere and hot coronal plasma, driven by downward heat conduction. Another stabilizer occurs when the heating $f(s)$ as a function of distance s along the loop does not fall off too dramatically with height. If it does, then cooling ensues and the system evolves dynamically as dynamic equilibrium is lost. Occasionally, specific formulations exhibit limit cycle behavior. Depending on initial states, a limit cycle solution and a different equilibrium solution might explain qualitatively our main results. The “0D” model Kuin & Martens (1982) exhibited such behavior, and tests revealed that the two kinds of solutions result from insufficient coupling between chromosphere and corona (see also van den Oord & Barstow 1988). Müller et al. (2003a) found limit cycle behavior in their 1D calculations of a short plasma loop, depending on the damping length k using a heating function $f(s) = \exp(-s/\ell)$.

Firmer conclusions are difficult to draw from these thermal models, in part because of the several ad-hoc assumptions behind them and the consequent large parameter space to be explored. Prescriptions based upon equation (8) amount to a “closure” of simplified equations of motion, determining all outcomes including those relevant for stability. They have no justification in terms of physical dissipation mechanisms within real plasmas. At this stage we therefore regard the question posed above as unanswered.

4.3.2. MHD and plasma processes

Here we follow the suggestion of LW93, and consider that a solution may be found among the physical heating mechanisms themselves. The authors, noting that almost all electrodynamic models of irreversible dissipative processes operate on unobservably small scales, nev-

ertheless concluded that such models could explain neither the observed intermittency nor the apparent transverse physical scale across plasma loops observable at the time.

Of all the irreversible processes discussed in section 3 of LW93, only their model of reconnection between adjacent, tangentially mis-aligned models might satisfy observed constraints. In particular the transverse thicknesses of plasma loops seemed to require interactions of elemental flux tubes (identified as such in the photosphere), essentially Parker’s (1988) picture of nanoflare heating. However, the lack of discrete tubes seen in modern observations of the solar photosphere suggests that elemental structures may consist of tortuous eddies of magnetic flux formed by convective dynamics (Rast et al. 2021). Such ideas are worth pursuing, especially with the new observational capabilities offered by DKIST.

The EUV instrument (Rochus et al. 2020) on the Solar Orbiter mission (Marsch et al. 2005; Marsden et al. 2013), currently achieves a similar resolution to that found by Rachmeler et al. (2022), close to 240 km. Further detailed studies of EUV data should thus be a priority, to explore these two pictures (ion viscosity versus topological change due to reconnection). A scale of 240 km is close to that at which ion-ion collisions (“viscosity”) can thermalize compressive motions (Hollweg 1986; Davila 1987; Judge & Ionson 2024), driven by a variety of processes which might include MHD turbulence, wave motions in inhomogeneous conditions and reconnection. Future studies might be able to rule out the viscous picture if scales well below, say, 200 km can be found within coronal loops, since then dissipation must occur on scales below the current observational horizon (Judge & Ionson 2024).

Intriguing behavior has been found in analytical (Uzdensky 2007) and numerical (Einaudi et al. 2021) studies of non linear plasma dynamics. Uzdensky (2007) appeals to a transition from slow to fast magnetic reconnection regimes according to whether coronal loop plasmas are collisional or collisionless systems. Einaudi et al. (2021) found in their MHD numerical turbulence experiment characteristics of a *self-regulating system*, in which the “state [of the plasma] occurs independently of the detailed form of the boundary velocity.” The driving energy used in their idealized “plasma loop” was about 3×10^5 erg cm⁻² s⁻¹, about 30 times smaller than requirements for active region plasma. They concluded that non-linear processes occurring within the corona itself determine the spatial and temporal properties within the fluid. Perhaps such effects, or similar non-linearities are necessary to organize coronal plasma

loops into macroscopic states which resemble the intermittently, but not randomly, ordered corona.

5. CONCLUSIONS

Coronal heating is and must always be an observationally-led research area. In the near future we anticipate the advent of further new idealized numerical experiments, novel data from observational facilities such as GREGOR and DKIST, and from instruments such as those on the Solar Orbiter spacecraft, which will help illuminate the problems raised in this study. Future observational work should attempt to understand the nature of unresolved motions in the upper chromosphere in relation to the long-lived magnetic fields there. POS motions and, if possible, POS chromospheric magnetic field components should also be included to study this problem. Measurements of magnetic fields from photosphere to coronal base should, assuming magnetic field line continuity, help resolve the ambiguity in the POS chromospheric magnetic field vector, by tracing fields from their single polarity roots into canopy-like configurations.

Given our assumptions, data and analysis, we are faced with a potential conundrum: What happens where there is clearly a signature of chromospheric Poynting flux but no coronal loop footpoints? Is there an unseen corona between the visible coronal loops? If indeed the chromospheric Poynting flux estimates with no associated visible coronal loop inject energy into the corona, where does it go? Does it escape to infinity or become

stored in the wider corona? Could the coronal heating be a secondary result of such processes?

The observations suggests that the “empty” corona between loops may be in a different, yet long-lived state. Otherwise we might argue that those “empty” loops would fill up with plasma, much like [Kuin & Martens \(1982\)](#) envisioned in their original model. Perhaps there is some sort of threshold for forming the hot coronal loops, as suggested by [LW93](#). The high threshold for onset of coronal heating above active regions ([LW93](#)) finds a natural explanation in the switch from slow fluid reconnection to fast collisionless reconnection, proposed by [Uzdensky \(2007\)](#). Future work on this proposal seems worthwhile. Scalings to conditions between main sequence and evolved stars do not discount this picture (work in progress).

As a final thought, this work reminds us to seek elementary and robust empirical facts about remotely sensed astronomical objects, before we throw the full machinery of numerical exploration, machine learning and advanced, detailed modeling at certain problems (see also [Judge & Ionson 2024](#)).

ACKNOWLEDGMENTS

The authors thanks Lucia Kleint and the astronomy department at the University of Bern and the Swiss National Science Foundation (grant No. 216870) which made this work possible. This material is based upon work supported by the National Center for Atmospheric Research, which is a major facility sponsored by the National Science Foundation under Cooperative Agreement No. 1852977. Comments from Peter Cargill and a patient anonymous referee greatly influenced this article, and are gratefully acknowledged.

APPENDIX

A. MULTIPOLAR CHROMOSPHERIC MAGNETIC FIELDS?

In this appendix we extend conceptual models of reconnection of multipolar photospheric fields as a driver of coronal heating of plasma loops, up into the chromosphere where our critical observations are made. Thus we give the models proposed by [Title & Schrijver \(1998\)](#); [Priest et al. \(2002\)](#); [Wang \(2016\)](#); [Chitta et al. \(2017, 2023\)](#). the benefit of the doubt, to see if they remain viable when confronted with chromospheric field measurements.

Unlike the photosphere, the measurements of chromospheric fields are from regions of $\beta \ll 1$, thus the field strengths $|\mathbf{B}|$ in such regions must locally be almost identical, independent of the direction of the field line vectors. Let us consider then the case where each observed pixel receives photons from a distribution of orientations of magnetic field vectors all with the same strength B_0 . Then the magnetic field inferred from the circularly polarized line profile (Stokes V) relative to intensity I yields, in each pixel,

$$B_{\text{LOS}} = \langle B_0 \cos \theta \rangle = \frac{B_0}{A} \int_A \cos \theta(x, y) dx dy. \quad (\text{A1})$$

Here x and y specify geometric coordinates in the plane perpendicular to the LOS, and A is the projected area of one detector pixel onto this plane. $0 \leq \theta \leq \pi$ are the (also unknown) angles of inclination of the fields to the line of sight

($\theta = 0$ being parallel to it, $\theta = \pi$ anti-parallel). In the text we find B_{LOS} is typically 250 Mx cm^{-2} , and is of the same sign beneath and in the neighborhood of each observed loop footpoint.

In the above equation, B_0 lies outside of the integral owing to the smallness of β . To illuminate implications of unresolved chromospheric magnetic fields of opposite polarity, we can assume that $\cos\theta$ under the integral has just two components, parallel and antiparallel to the LOS, which reconnect, releasing magnetic free energy for subsequent heating. Then

$$B_{\text{LOS}} = B_0(1 - f - f) = B_0(1 - 2f) \quad (\text{A2})$$

where $f < 0.5$ is the fractional area of the minority component. When $f \ll 1$, the measured $B_{\text{LOS}} \rightarrow B_0$. In the other limit where $f = 1/2 - \delta$, $\delta \ll 1$, $B_{\text{LOS}} \rightarrow B_0\delta \ll B_0$. Next let us assume, as argued by those advocating for multipolar fields as agents of heating, that each loop footpoint sits above a case where f is finite, and that outside each footpoint f is negligibly small. The basic observational fact from our analysis in the text is that B_{LOS} is roughly constant, say B_1 , across the loop footpoint and its immediate surroundings. A clear example is shown in in Figure 6 of J24a, in the neighborhood of the bright EUV footpoint at $X = -403$, $Y = -385$. Within those pixels with mixed LOS polarity we have $B_{\text{LOS,mixed}} = B_1 = B_0\delta$. Outside this region where δ is negligible, we have $B_{\text{LOS,unipolar}} = B_1 = B_0$. The data show that $B_{\text{LOS,mixed}} \approx B_{\text{LOS,unipolar}}$, so that we arrive at $B_0 = B_0\delta$, which is a contradiction since $0 \leq \delta \leq 1/2$.

This argument is supported by noting that any reconnection associated with the annihilation of opposite polarity fields should be accompanied by Doppler signatures of vertical motions $u \lesssim c_A \approx 1000 \text{ km s}^{-1}$ in the upper chromosphere. Yet the movie (Figure 6 of J24b) of $\text{H}\alpha$ core intensities shows no indication of changes of magnetic connectivity in the upper chromosphere during the duration of the GRIS observations. Further, observed spectral linewidths and shifts of chromospheric and coronal lines are typically two orders of magnitude smaller. (see Appendix A of Judge & Ionson 2024).

We conclude that it does not seem possible to heat the loops associated with unipolar regions by invoking the reconnection of minority polarity fields lying below current limits of observability, without violating some basic observational constraints. Instead, solutions must be sought based upon locally unipolar fields (Judge 2021).

REFERENCES

- Aschwanden, M. J., Nightingale, R. W., & Alexander, D. 2000, *ApJ*, 541, 1059
- Aschwanden, M. J., Winebarger, A., Tsiklauri, D., & Peter, H. 2007, *ApJ*, 659, 1673
- Athay, R. G. 1976, *The Solar Chromosphere and Corona: Quiet Sun* (Dordrecht: Reidel)
- Avrett, E. H., Fontenla, J. M., & Loeser, R. 1994, in *Infrared Solar Physics*, ed. D. M. Rabin, J. T. Jefferies, & C. Lindsey, *Proc. IAU Symp.* 154 (Dordrecht: Kluwer), 35–47t
- Barczynski, K., Peter, H., Chitta, L. P., & Solanki, S. K. 2018, *A&A*, 619, A5, doi: [10.1051/0004-6361/201731650](https://doi.org/10.1051/0004-6361/201731650)
- Beliën, A. J. C., Martens, P. C. H., & Keppens, R. 1999, *ApJ*, 526, 478, doi: [10.1086/307980](https://doi.org/10.1086/307980)
- Boris, J. P., & Mariska, J. T. 1982, *ApJL*, 258, L49, doi: [10.1086/183828](https://doi.org/10.1086/183828)
- Bradshaw, S. J., & Cargill, P. J. 2013, *ApJ*, 770, 12, doi: [10.1088/0004-637X/770/1/12](https://doi.org/10.1088/0004-637X/770/1/12)
- Bradshaw, S. J., & Mason, H. E. 2003, *A&A*, 401, 699, doi: [10.1051/0004-6361:20030089](https://doi.org/10.1051/0004-6361:20030089)
- Braginskii, S. I. 1965, *Reviews of Plasma Physics.*, 1, 205
- Cargill, P. J., Bradshaw, S. J., & Klimchuk, J. A. 2012a, *ApJ*, 758, 5, doi: [10.1088/0004-637X/758/1/5](https://doi.org/10.1088/0004-637X/758/1/5)
- . 2012b, *ApJ*, 752, 161, doi: [10.1088/0004-637X/752/2/161](https://doi.org/10.1088/0004-637X/752/2/161)
- Cauzzi, G., Reardon, K. P., Uitenbroek, H., et al. 2008, *A&A*, 480, 515
- Chitta, L. P., Peter, H., & Young, P. R. 2016, *A&A*, 587, A20, doi: [10.1051/0004-6361/201527340](https://doi.org/10.1051/0004-6361/201527340)
- Chitta, L. P., Peter, H., Solanki, S. K., et al. 2017, *ApJS*, 229, 4, doi: [10.3847/1538-4365/229/1/4](https://doi.org/10.3847/1538-4365/229/1/4)
- Chitta, L. P., Solanki, S. K., del Toro Iniesta, J. C., et al. 2023, *ApJL*, 956, L1, doi: [10.3847/2041-8213/acf136](https://doi.org/10.3847/2041-8213/acf136)
- Collados, M., López, R., Páez, E., et al. 2012, *Astronomische Nachrichten*, 333, 872, doi: [10.1002/asna.201211738](https://doi.org/10.1002/asna.201211738)
- Craig, I. J. D. 1990, *A&A*, 234, L12
- Craig, I. J. D., & Scholtes, R. M. S. M. 1985, *ApJ*, 296, 710, doi: [10.1086/163488](https://doi.org/10.1086/163488)
- Cranmer, S. R., & Molnar, M. E. 2023, *ApJ*, 955, 68, doi: [10.3847/1538-4357/acee6c](https://doi.org/10.3847/1538-4357/acee6c)
- Davila, J. M. 1987, *ApJ*, 317, 514
- de Wijn, A. G., Casini, R., Carlile, A., et al. 2022, *Solar Phys.*, 297, 22
- Einaudi, G., Dahlburg, R. B., Ugarte-Urra, I., et al. 2021, *ApJ*, 910, 84

- Foukal, P. 1975, *Sol. Phys.*, 43, 327
- Foukal, P. 1976, *ApJ*, 210, 575
- Golub, L., Maxson, C., Rosner, R., Vaiana, G. S., & Serio, S. 1980, *ApJ*, 238, 343, doi: [10.1086/157990](https://doi.org/10.1086/157990)
- Grec, C., Uitenbroek, H., Faurobert, M., & Aime, C. 2010, *A&A*, 514, A91, doi: [10.1051/0004-6361/200811455](https://doi.org/10.1051/0004-6361/200811455)
- Hansteen, V. 1993, *ApJ*, 402, 741
- Hoeksema, J. T., Baldner, C. S., Bush, R. I., Schou, J., & Scherrer, P. H. 2018, *Sol. Phys.*, 293, 45, doi: [10.1007/s11207-018-1259-8](https://doi.org/10.1007/s11207-018-1259-8)
- Hollweg, J. V. 1986, *ApJ*, 306, 730
- Howson, T. A., de Moortel, I., & Reid, J. 2020, *A&A*, 636, A40
- Ionson, J. A. 1978, *ApJ*, 226, 650
- Jordan, C., Ayres, T. R., Brown, A., Linsky, J. L., & Simon, T. 1987, *MNRAS*, 225, 903, doi: [10.1093/mnras/225.4.903](https://doi.org/10.1093/mnras/225.4.903)
- Jordan, C., Mendoza, B., & Gill, R. S. 1984, in *ESA-SP 220*, ed. T. D. Guyenne & J. J. Hunt (ESA), 133–136
- Judge, P., Kleint, L., Casini, R., et al. 2024a, *ApJ*, 960, 129
- Judge, P., Kleint, L., & Kuckein, C. 2024b, *ApJ* submitted, February 2024
- Judge, P. G. 2021, *ApJ*, 914, 70
- Judge, P. G., & Ionson, J. A. 2024, *The Problem of Coronal Heating. A Rosetta Stone for Electrodynamical Coupling in Cosmic Plasma* (Springer, in press, March 2024)
- Judge, P. G., Kleint, L., Donea, A., Sainz Dalda, A., & Fletcher, L. 2014, *ApJ*, 796, 85
- Kleint, L., Berkefeld, T., Esteves, M., et al. 2020, *A&A*, 641, A27, doi: [10.1051/0004-6361/202038208](https://doi.org/10.1051/0004-6361/202038208)
- Klimchuk, J. A. 2006, *Solar Phys.*, 234, 41
- Klimchuk, J. A., Patsourakos, S., & Cargill, P. J. 2008, *ApJ*, 682, 1351, doi: [10.1086/589426](https://doi.org/10.1086/589426)
- Krieger, A. S., Vaiana, G. S., & van Speybroeck, L. P. 1971, in *Solar Magnetic Fields*, ed. R. Howard, Vol. 43 (*Proc. IAU*), 397–412
- Kuin, N. P. M., & Martens, P. C. H. 1982, *A&A*, 108, L1
- Leenaarts, J., Carlsson, M., Hansteen, V., & Rouppe van der Voort, L. 2009, *ApJL*, 694, L128
- Leenaarts, J., Golding, T., Carlsson, M., Libbrecht, T., & Joshi, J. 2016, *A&A*, 594, A104
- Lemen, J., Title, A., de Pontieu, B., et al. 2011, in *AAS/Solar Physics Division Abstracts #42*, Vol. 289, 1512
- Lemen, J. R., Title, A. M., Akin, D. J., et al. 2012, *Sol. Phys.*, 275, 17, doi: [10.1007/s11207-011-9776-8](https://doi.org/10.1007/s11207-011-9776-8)
- Linsky, J. L., & Avrett, E. H. 1970, *PASP*, 82, 169
- Litwin, C., & Rosner, R. 1993, *ApJ*, 412, 375
- López Fuentes, M., & Klimchuk, J. A. 2022, *ApJ*, 939, 17, doi: [10.3847/1538-4357/ac90c8](https://doi.org/10.3847/1538-4357/ac90c8)
- Malanushenko, A., Cheung, M. C. M., DeForest, C. E., Klimchuk, J. A., & Rempel, M. 2022, *ApJ*, 927, 1
- Mariska, J. T., Doschek, G. A., Boris, J. P., Oran, E. S., & Young, T. R., J. 1982, *ApJ*, 255, 783, doi: [10.1086/159877](https://doi.org/10.1086/159877)
- Marsch, E., Marsden, R., Harrison, R., Wimmer-Schweingruber, R., & Fleck, B. 2005, *Advances in Space Research*, 36, 1360
- Marsden, R. G., Müller, D., & StCyr, O. C. 2013, in *American Institute of Physics Conference Series*, Vol. 1539, *Solar Wind 13*, ed. G. P. e. a. Zank, 448–453
- Martens, P. C. H. 2010, *ApJ*, 714, 1290, doi: [10.1088/0004-637X/714/2/1290](https://doi.org/10.1088/0004-637X/714/2/1290)
- McClymont, A. N., & Craig, I. J. D. 1985a, *ApJ*, 289, 820, doi: [10.1086/162946](https://doi.org/10.1086/162946)
- . 1985b, *ApJ*, 289, 834, doi: [10.1086/162947](https://doi.org/10.1086/162947)
- Müller, D. A. N., Hansteen, V. H., & Peter, H. 2003a, *A&A*, 411, 605
- Müller, W.-C., Biskamp, D., & Grappin, R. 2003b, *PhRvE*, 67, 066302
- Parker, E. N. 1988, *ApJ*, 330, 474
- Patsourakos, S., & Klimchuk, J. A. 2005, *ApJ*, 628, 1023, doi: [10.1086/430662](https://doi.org/10.1086/430662)
- Pesnell, W. D., Thompson, B. J., & Chamberlin, P. C. 2012, *Sol. Phys.*, 275, 3
- Pevtsov, A. A., Fisher, G. H., Acton, L. W., et al. 2003, *ApJ*, 598, 1387
- Poletto, G., Vaiana, G. S., Zombeck, M. V., Krieger, A. S., & Timothy, A. F. 1975, *Sol. Phys.*, 44, 83, doi: [10.1007/BF00156848](https://doi.org/10.1007/BF00156848)
- Priest, E. R., Heyvaerts, J. F., & Title, A. M. 2002, *ApJ*, 576, 533
- Rachmeler, L. A., Bueno, J. T., McKenzie, D. E., et al. 2022, *ApJ*, 936, 67, doi: [10.3847/1538-4357/ac83b8](https://doi.org/10.3847/1538-4357/ac83b8)
- Rast, M. P., Bello González, N., Bellot Rubio, L., et al. 2021, *Sol. Phys.*, 296, 70, doi: [10.1007/s11207-021-01789-2](https://doi.org/10.1007/s11207-021-01789-2)
- Rimmele, T. R., Warner, M., Keil, S. L., et al. 2020, *Sol. Phys.*, 295, 172, doi: [10.1007/s11207-020-01736-7](https://doi.org/10.1007/s11207-020-01736-7)
- Rochus, P., Auchère, F., Berghmans, D., et al. 2020, *A&A*, 642, A8, doi: [10.1051/0004-6361/201936663](https://doi.org/10.1051/0004-6361/201936663)
- Rosner, R. 1990, in *Physics of Magnetic Flux Ropes*, ed. C. T. Russell, E. R. Priest, & L. C. Lee, Vol. 58 (*Washington DC American Geophysical Union Geophysical Monograph Series*), 189, doi: [10.1029/GM058](https://doi.org/10.1029/GM058)
- Rosner, R., Tucker, W. H., & Vaiana, G. S. 1978, *ApJ*, 220, 643
- Schmidt, W., von der Lühe, O., Volkmer, R., et al. 2012, *Astronomische Nachrichten*, 333, 796, doi: [10.1002/asna.201211725](https://doi.org/10.1002/asna.201211725)

- Schrijver, C. J., & Harvey, K. L. 1989, *ApJ*, 343, 481
- Schrijver, C. J., & Zwaan, C. 2000, *Solar and Stellar Magnetic Activity* (New York: Cambridge University Press)
- Title, A. M., & Schrijver, C. J. 1998, in *Astronomical Society of the Pacific Conference Series*, Vol. 154, *Cool Stars, Stellar Systems, and the Sun*, ed. R. A. Donahue & J. A. Bookbinder, 345
- Toriumi, S., & Airapetian, V. S. 2022, *ApJ*, 927, 179, doi: [10.3847/1538-4357/ac5179](https://doi.org/10.3847/1538-4357/ac5179)
- Uzdensky, D. A. 2007, *ApJ*, 671, 2139, doi: [10.1086/522915](https://doi.org/10.1086/522915)
- van den Oord, G. H. J., & Barstow, M. A. 1988, *A&A*, 207, 89
- van Speybroeck, L. P., Krieger, A. S., & Vaiana, G. S. 1970, *Nat.*, 227, 818
- Vernazza, J., Avrett, E., & Loeser, R. 1981, *ApJS*, 45, 635
- Wang, Y. M. 2016, *ApJL*, 820, L13, doi: [10.3847/2041-8205/820/1/L13](https://doi.org/10.3847/2041-8205/820/1/L13)
- Wentzel, D. G. 1978, *SP*, 58, 307